Rational Design of Higher Conductivity Solid Oxide Electrolyte

Eric D. Wachsman (PI)
Juan C. Nino (Co-PI)
Simon R. Phillpot (Co-PI)
Susan B. Sinnott (Co-PI)

Materials Science and Engineering Department
University of Florida

Start Date = January 2005
Planned Completion = March 2007

Research Goals and Objectives

- *Computationally* determine the role of size difference, polarizability and dopant charge on vacancy cluster formation in Bi_2O_3
  - Characterize oxygen transport using atomic-level simulation
  - Identify the structure of oxygen defect clusters and determine their role in reducing ionic conductivity
- *Experimentally* determine the role of size difference, polarizability and dopant charge on vacancy cluster formation in Bi_2O_3
  - Prepare DWSB and determine conductivity as a function of total and relative dopant concentration
- Establish doping strategies to mitigate detrimental effects of vacancy clustering
- Apply knowledge to Ceria
  - Investigate co-doping effects on the ionic conductivity of ceria-based electrolytes
  - Compare the above results with the ionic conductivity of singly doped ceria in terms of critical ionic radius and polarizibility of dopant

Relevance to Current State-of-the-Art

Higher ionic conductivity electrolytes will:

- Reduce SOFC operating temperature
- Reduce SOFC cost
- Permit higher power density SOFCs

Relevance to NASA

Higher ionic conductivity electrolytes:

- Are essential to achieve NASA's goal of high power density fuel cells
- Will permit more efficient COG's for *ISRU* and life support applications

Budget, Schedule and Deliverables

- Budget: $210K + $210K

- Schedule:
- Q1 Four probe and impedance characterization of (Lu,Nd) doped Ceria as a function of temperature
- Q2 Elucidate point-defect migration mechanisms and the structure of defect clusters in Bi_2O_3
- Q3 Complete synthesis and characterization of Nd doped Ceria and comparison with previous analyzed systems to establish the individual effect of polarization and ionic radius
- Q4 Identify doping strategies to maximize ionic transport in Bi_2O_3 by studying the effects of the substitution of Bi ions by other trivalent atoms, such as Gd and Dy, and by with "artifical dopants" with atomic radii and polarizabilities that we can control independently
- Q5 Synthesize and characterize doped Ceria systems with constant effective critical dopant radius to analyze and separate the effect of polarizability
- Q6 Measure conductivity of new synthesized compounds as function of temperature and P_{O2}

- Deliverable: Higher conductivity solid oxide electrolyte

Anticipated Technology End Use

- Electric power generation:
  - Distributed generation
  - Auxillary Power Unit (APU)
- Life support and *ISRU*:
  - Ceramic oxygen generator

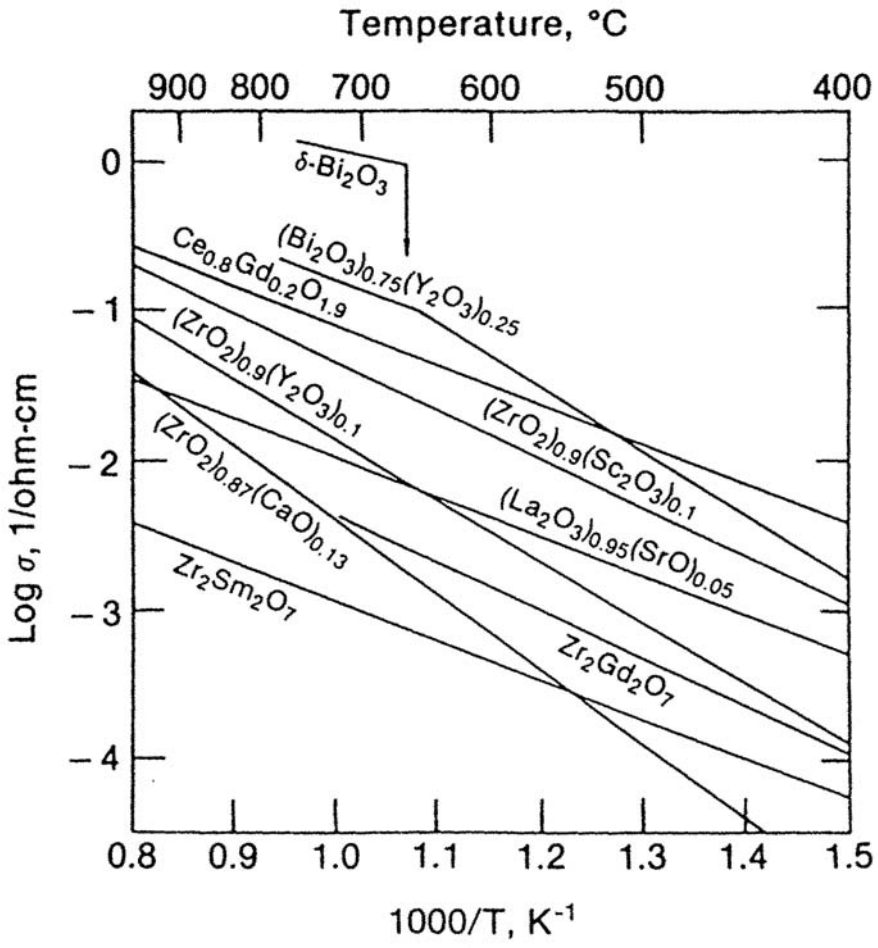

Figure 6.12 Examples of ceramics that have high oxygen ion conductivity. (After B. C. H. Steele, Ceramic materials for electrochemical energy conversion devices, *Ceramics in Advanced Energy Technologies*, D. Reidel, Dordrecht, 1984, pp. 386–412.)

$$\sigma_i = z_i q\, u_i\, [\, i\,]$$

z_i = charge of species "i"

q = charge of an electron

u_i = mobility of species "i"

$[\, i\,]$ = concentration of species "i"

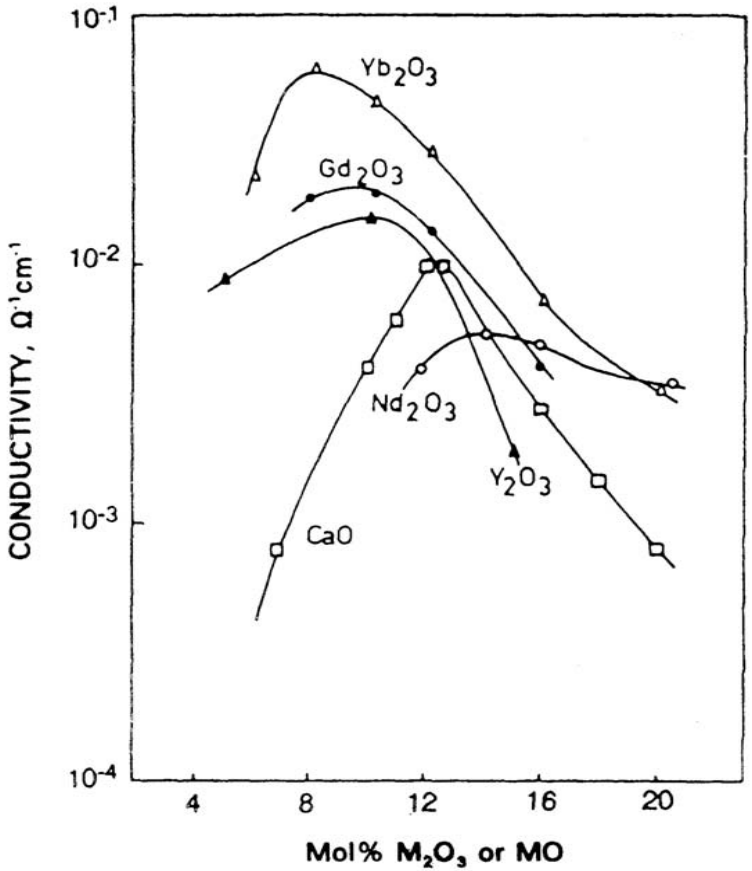

Figure 4.8. Variation of ionic conductivity of stabilized ZrO_2 with dopant concentration at 1080 K [4.65]

Conductivity

- increases with increasing dopant and thus $V_O^{\bullet\bullet}$ concentration at low <10% dopant level

- decreases at higher concentration due to defect association

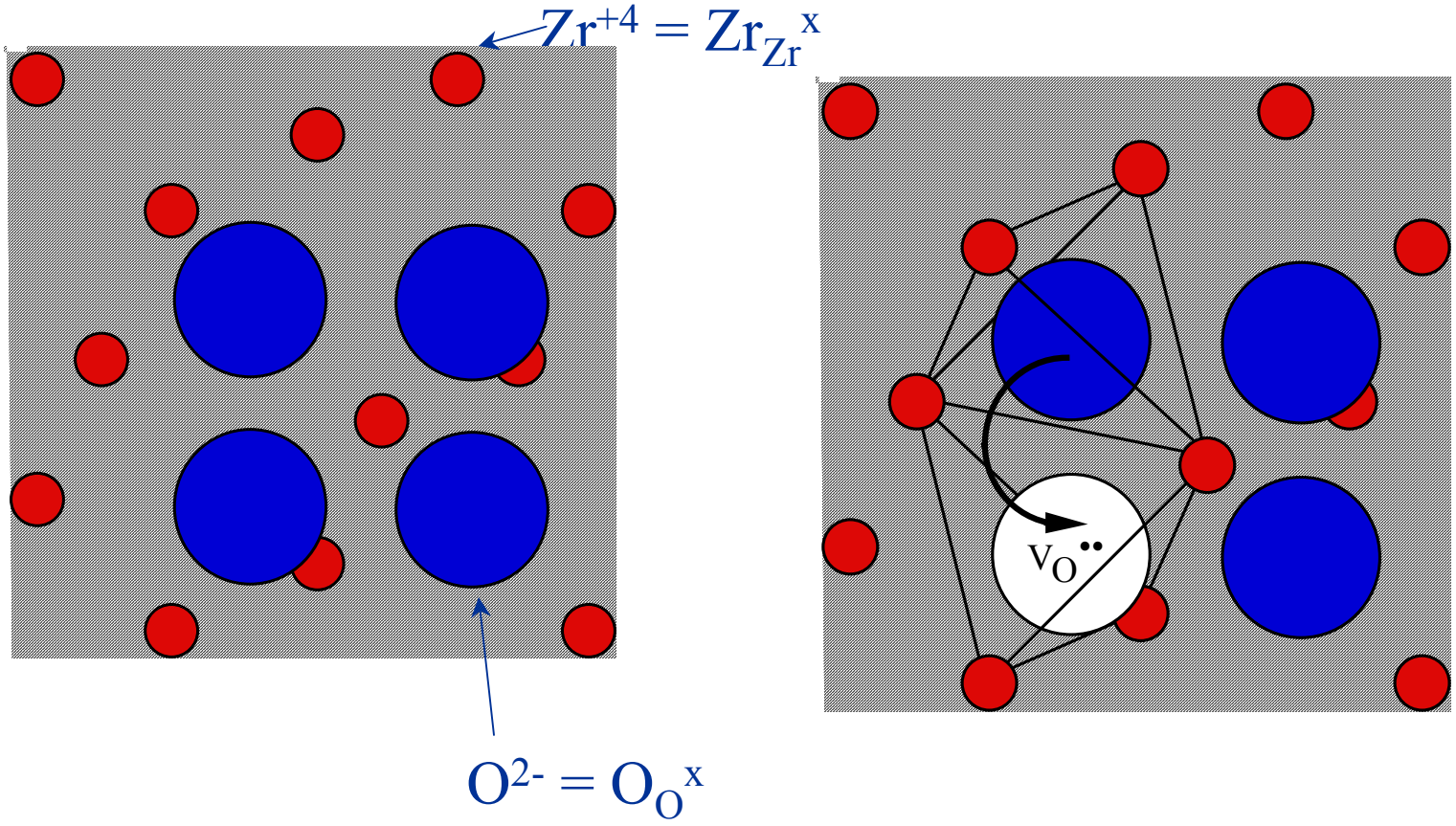

Anions in 4-fold coordination

Cations in 8-fold coordination

- but Zr likes to be in 6-fold coordination - elastic strain

Ordered Structure

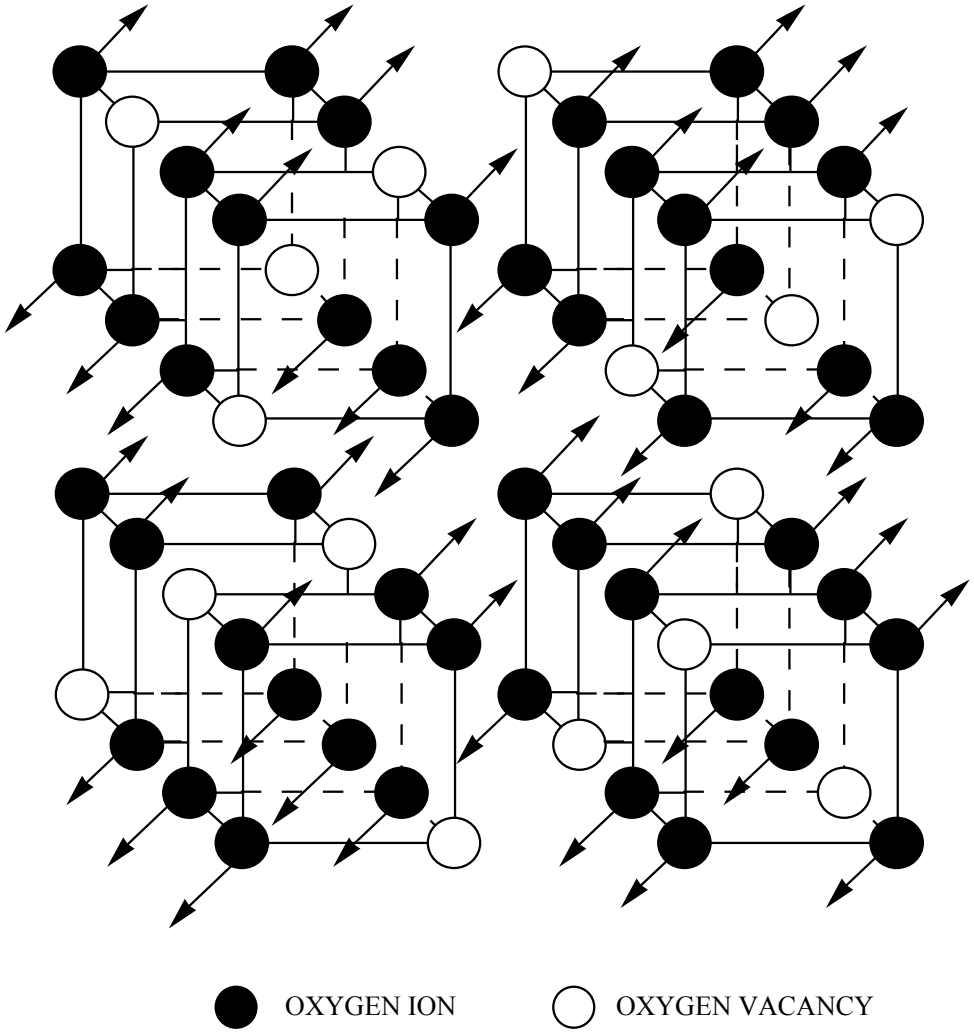

Disordered Structure

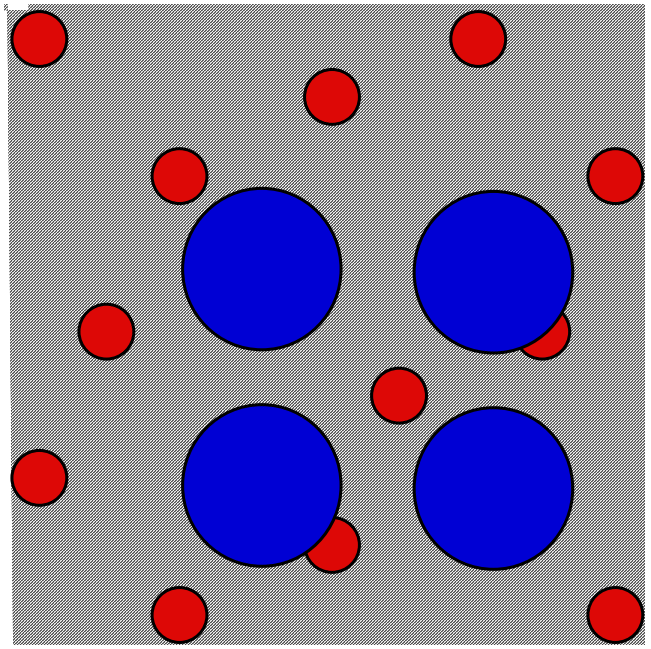

Table 7. Calculated Pre-Exponentials for Unaged and Aged $(Bi_2O_3)_{0.75}(M_2O_3)_{0.25}$

Dopant	$A_{Disordered\ Structure}$ x10^5 S cm^{-1} K	$A_{Ordered\ Structure}$ x10^5 S cm^{-1} K	$\frac{A_{Ordered\ Structure}}{A_{Disordered\ Structure}}$
Yb	34.33	2.40	0.069
Er	36.36	2.46	0.067
Y	44.35	3.02	0.068
Ho	37.61	2.72	0.072
Dy	38.44	3.54	0.092

Table 8. Measured Pre-exponentials for Unaged and Aged $(Bi_2O_3)_{0.75}(M_2O_3)_{0.25}$

Dopant	$A_{Disordered\ Structure}$ x10^5 S cm^{-1} K	$A_{Ordered\ Structure}$ x10^5 S cm^{-1} K	$\frac{A_{Ordered\ Structure}}{A_{Disordered\ Structure}}$
Yb	93.88	6.73	0.071
Er	52.39	1.98	0.037
Y	114.78	9.54	0.083
Ho	42.45	3.59	0.084
Dy	62.67	4.89	0.078

$$A = n\lambda^2 (ze)^2 \nu c_i / 6Vk$$

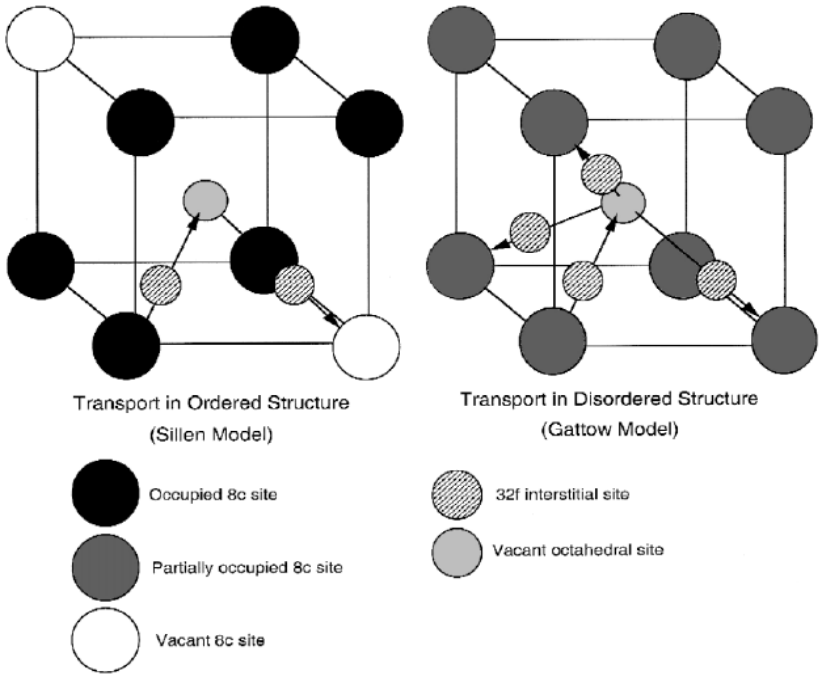

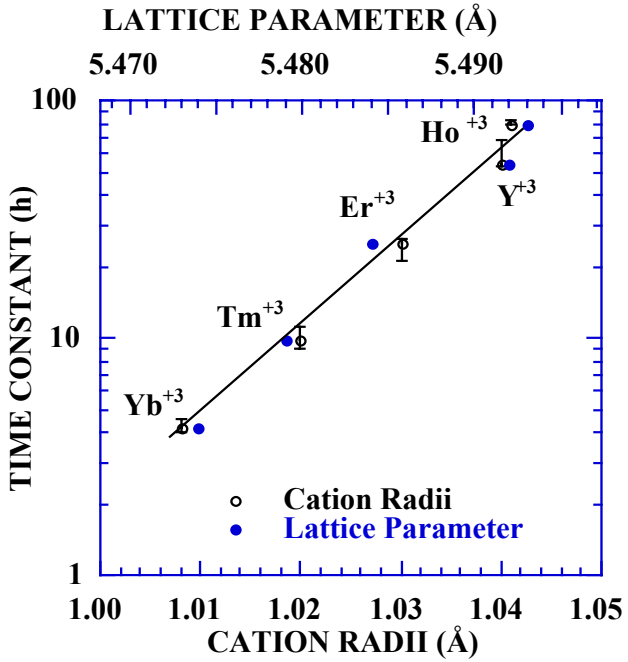

Time constant as a function of dopant cation radii and resultant lattice parameter in 25MSB.

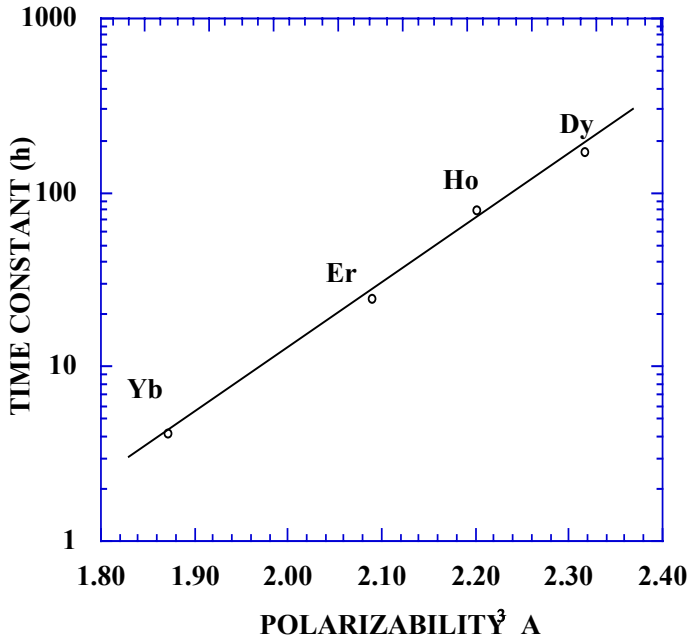

Time constant for aging as a function of dopant polarizability

- Anion ordering depends on dopant radii
- Dopant polarizability linearly related to radii

Conductivity of Bi_2O_3 With Highly Polarizable Dopants

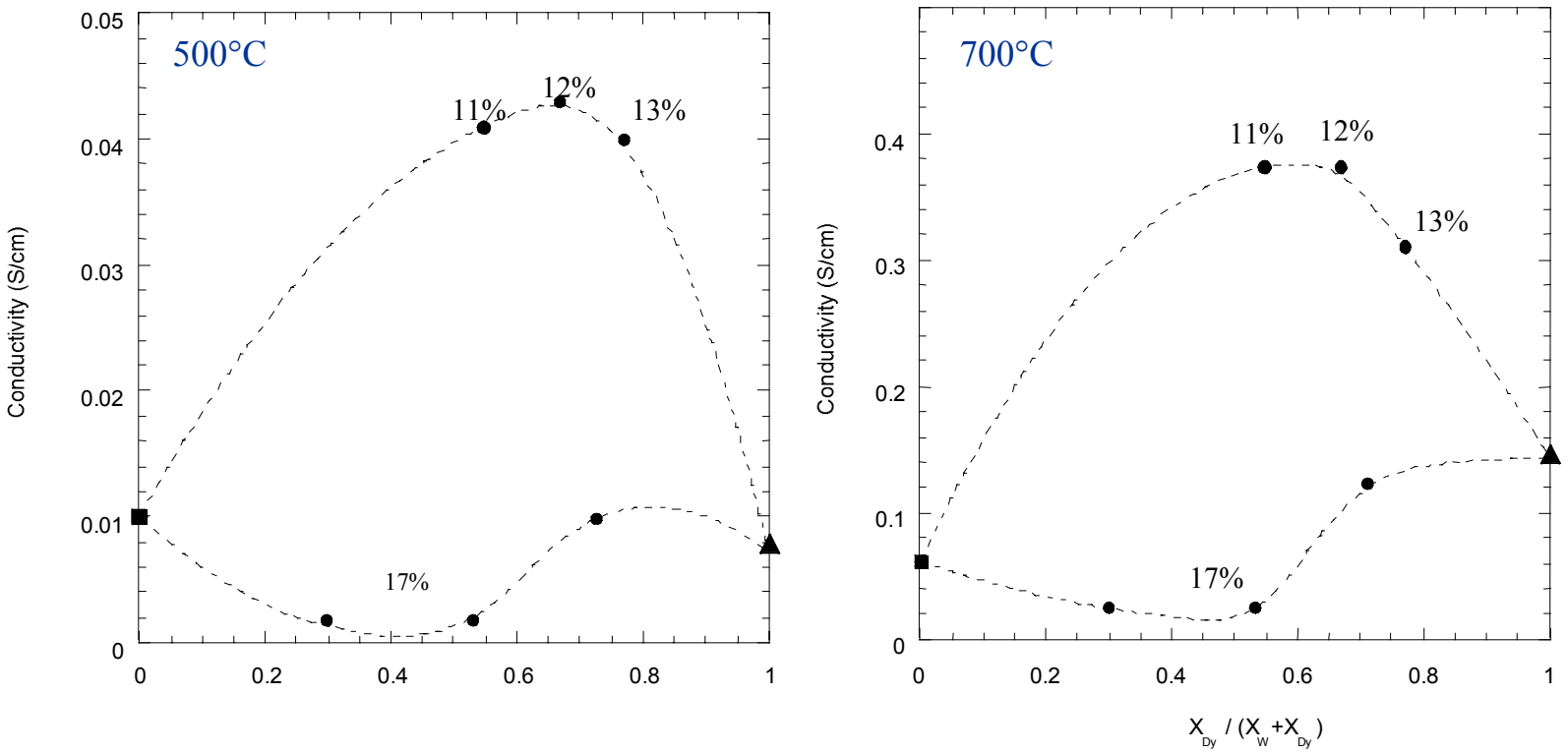

- Double doping with Dy and W is non-ideal
  - low concentration (~12%) maxima
  - Higher concentration (17%) minima

Atomic-Level Simulation Approach

- Molecular-dynamics simulation

- Bi and O interact via Coulombic forces and short-ranged mainly repulsive interaction
  - Specific interatomic-description developed by Jacobs and MacDonaill (Solid State Ionics **23** 279 (1987)

- Good agreement with experiment for d-Bi_2O_3

	Experiment	Simulation
Lattice Constant (Angstrom)	5.644	5.644
ε_o (α –phase)	18.2	18.78
$\alpha_{O^{2-}}$ (A^3)	3.92	3.927

Accomplishments and Results

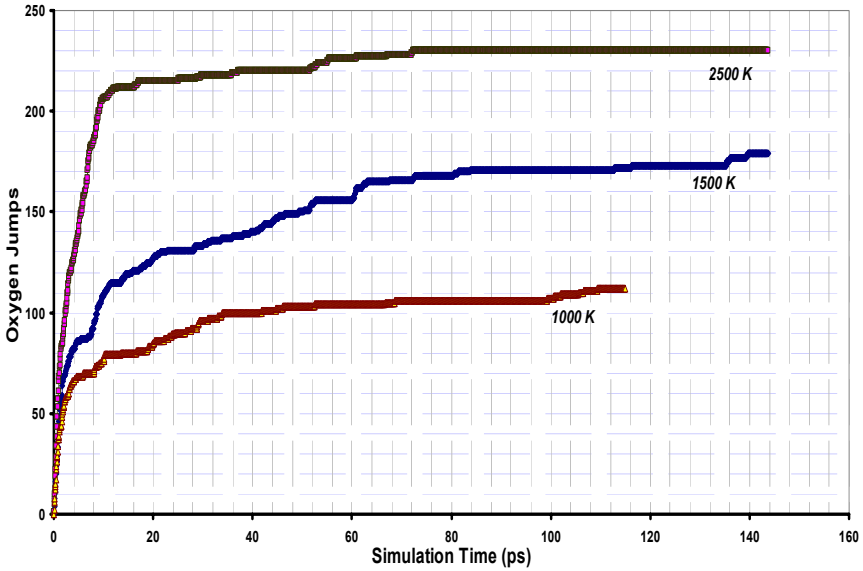

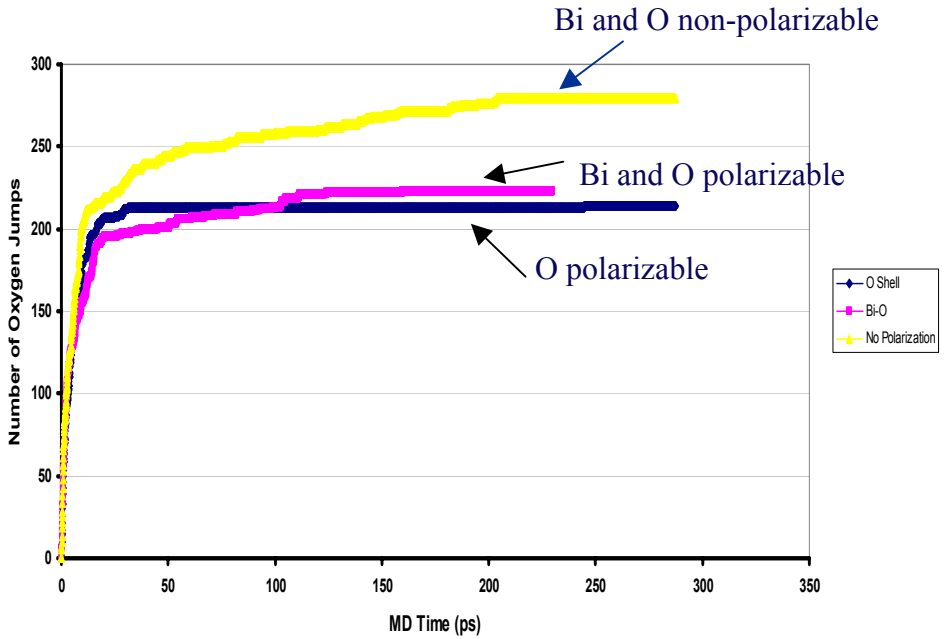

- Oxygen migration:
  - -decreases with time
  - -increases with temperature
- Consistent with development of low-mobility vacancy cluster

- Ion polarizability enables more rapid structural equilibrium

Accomplishments and Results

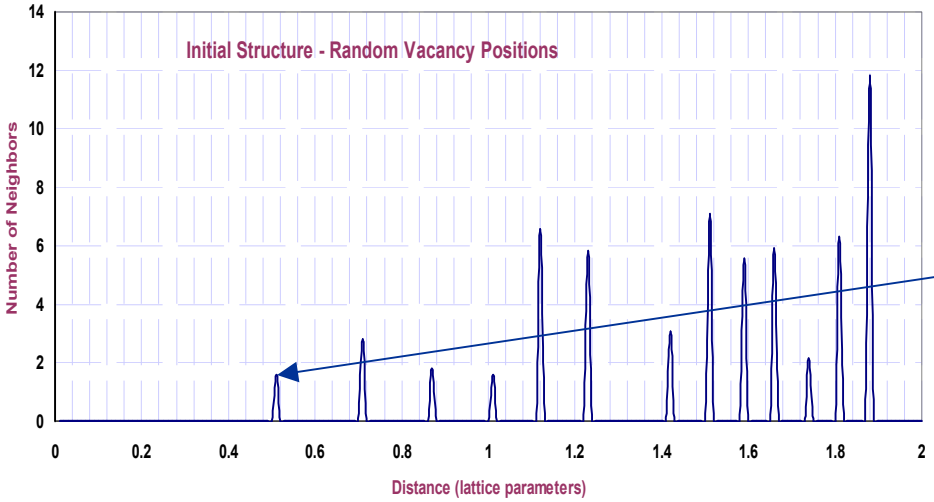

Input structure for simulation – vacancies randomly placed/

- Nearest neighbor peak at 0.5a –neighbors in <100> directions

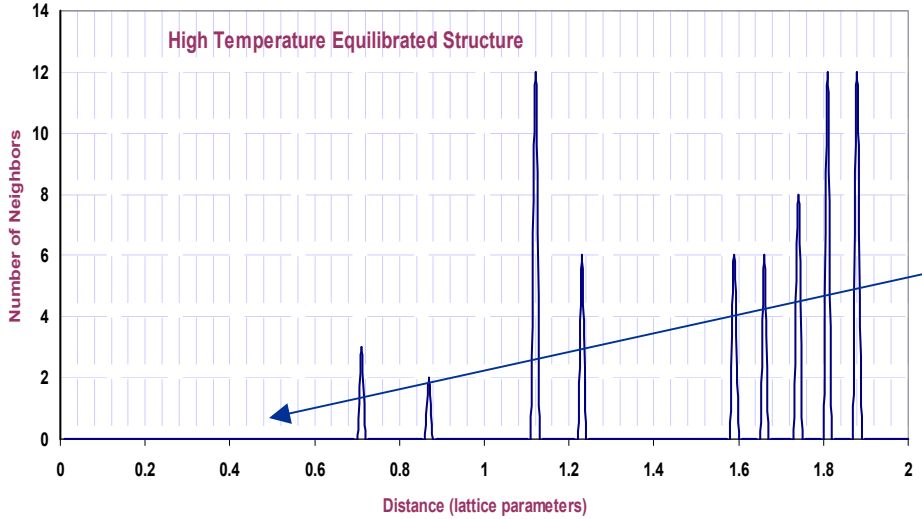

After equilibration at high temperature

-Vacancies redistribute to form vacancy lattice
- no vacancy-vacancy nearest neighbors in the <100> directions
- strong ordering of vacancies in <110> and <110> directions

Accomplishments and Results

Vacancy Ordering in Bi_2O_3

All vacancies in the equilibrated structure are in identical environments:

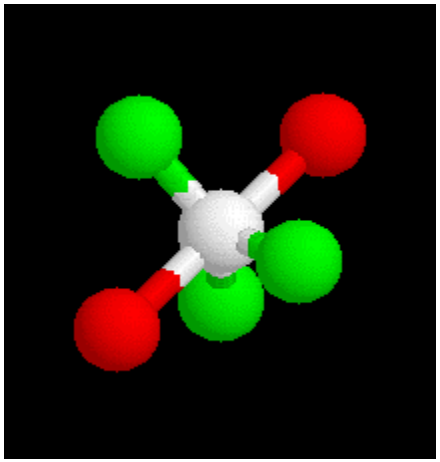

Three second neighbors in <110> directions form a plane with central vacancy

Two third neighbors in <111> direction make a line with the central vacancy

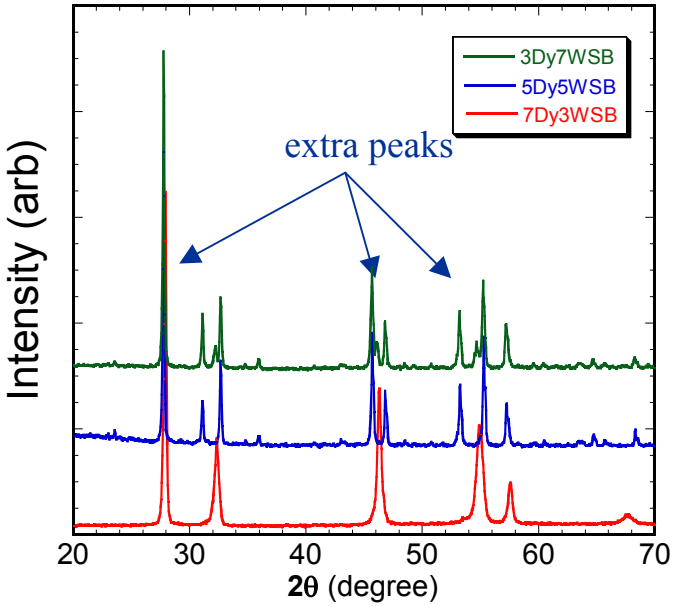

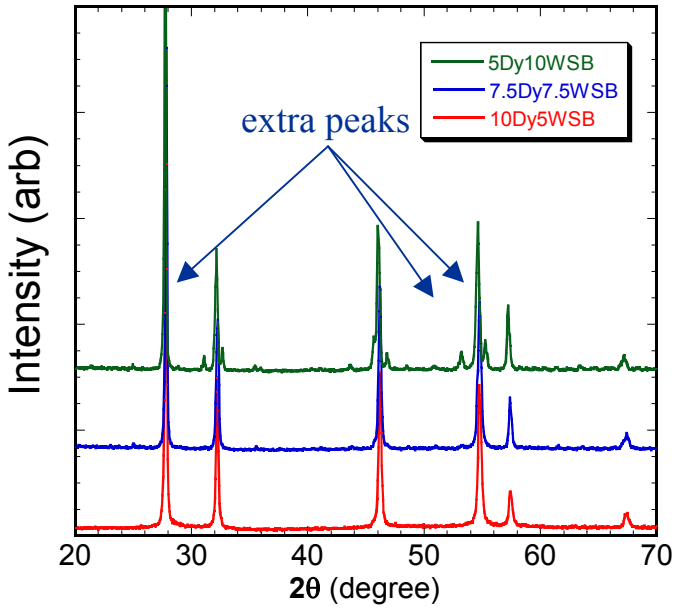

Total dopant conc. 10 mol.%	Total dopant conc. 15 mol.%
7Dy3WSB	Single phase
5Dy5WSB	Mixed phase
3Dy7WSB	Mixed phase
10Dy5WSB	Single phase
7.5Dy7.5WSB	Single phase
5Dy10WSB	Mixed phase

Accomplishments and Results

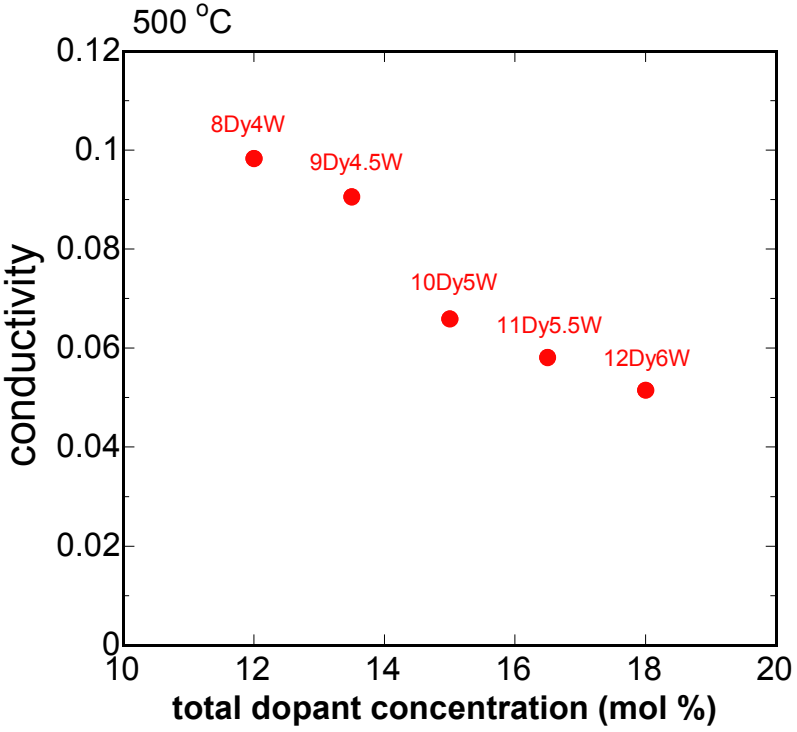

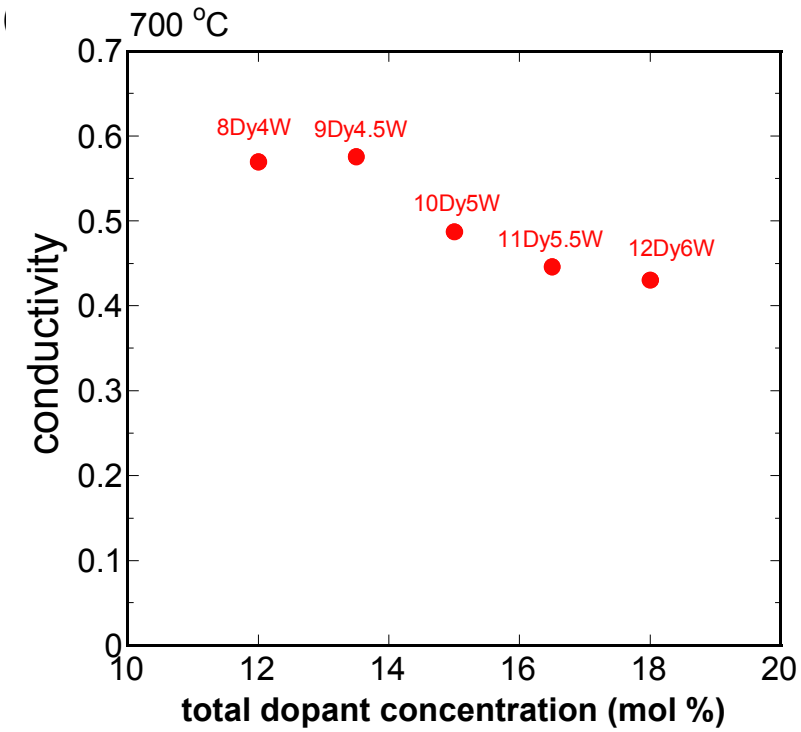

The conductivity increases as total dopant concentration decreases

Consistent with singly doped Bi_2O_3 trend in literature

Conductivity of Bi_2O_3 With Highly Polarizable Dopants

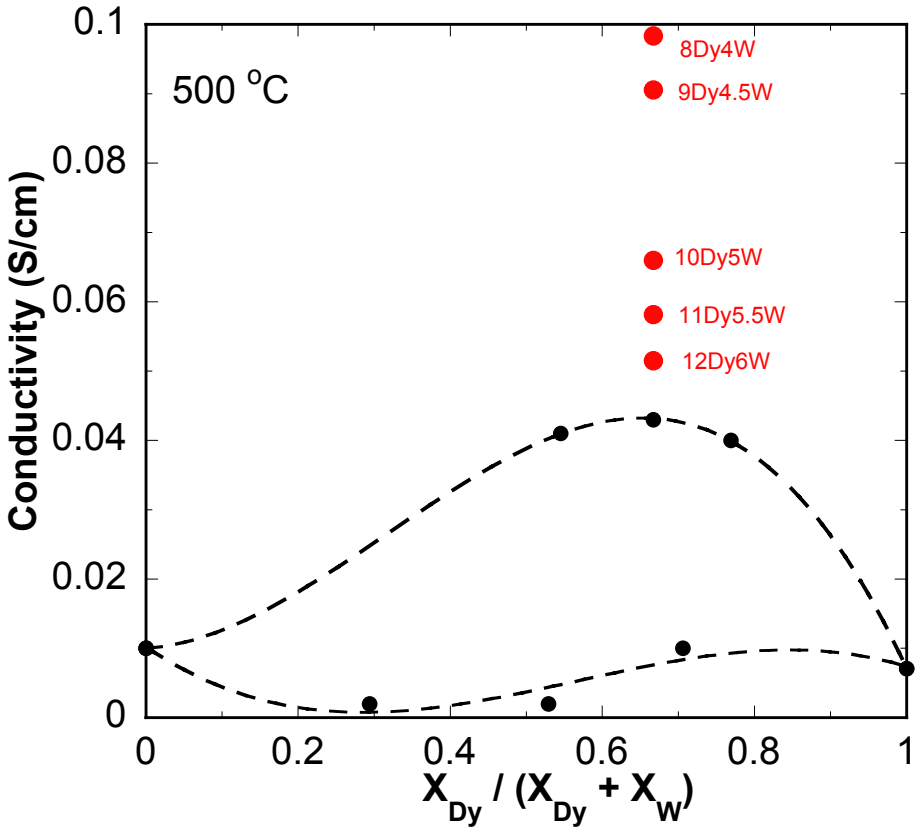

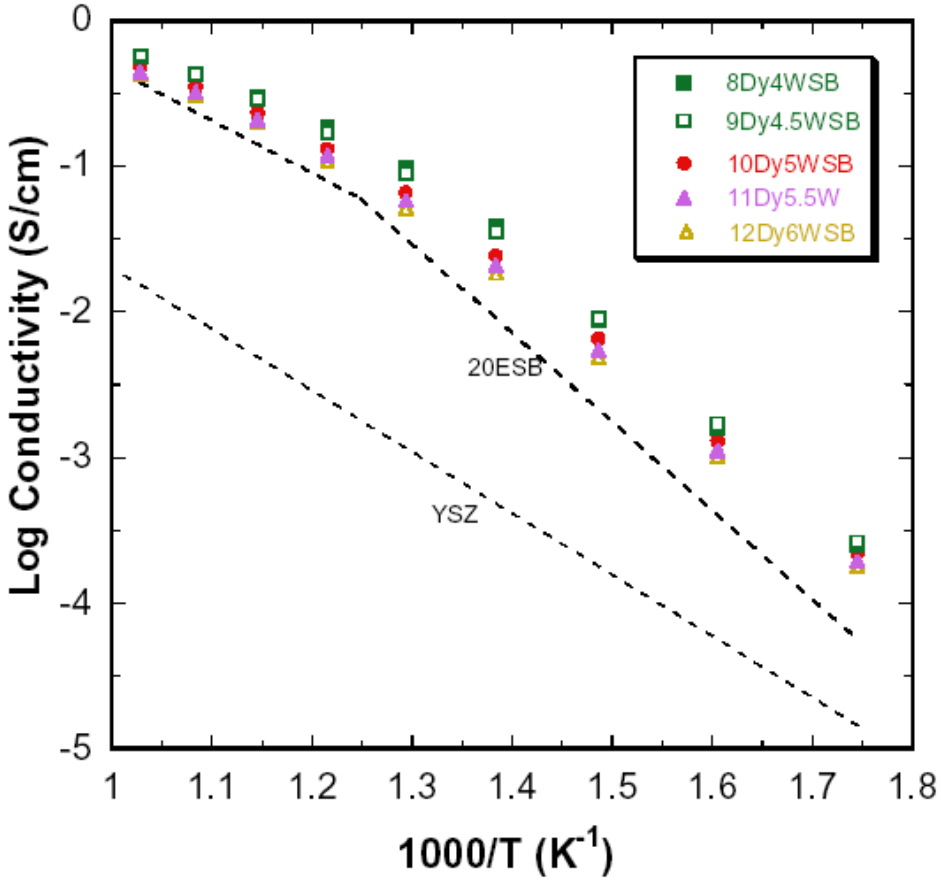

- 4X conductivity of ESB
- 200X conductivity of YSZ

Critical Ionic Radius (r_c)

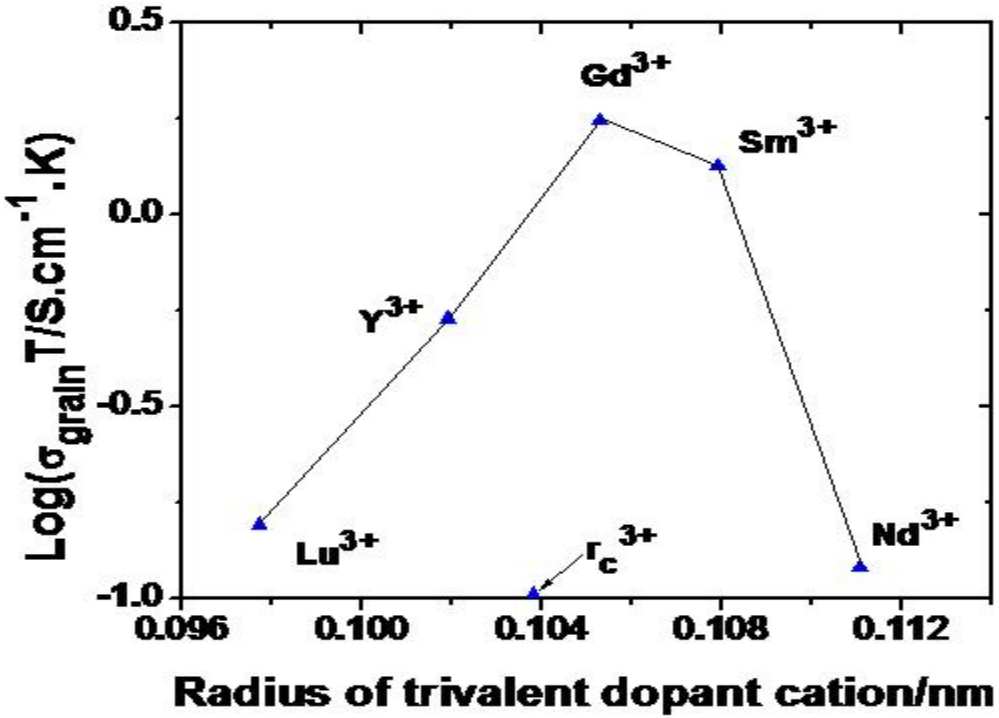

Critical ionic radius is defined as the ionic radius of the dopant that neither causes expansion nor contraction of the host fluorite lattice[1].

$r_c^{3+} = 1.038$ Å

$r^{3+}_{Gd,VIII} = 1.053$ Å

Bulk ionic conductivity at 400°C as a function of trivalent dopant radii[2-5]

1. D. J. Kim, J. Am. Ceram. Soc. 72 (1989) 1415
2. Liping Li, Xiaomin Lin, Guangshe Li, Hiroshi Inomata, J. Mater. Res., Vol 16, No.11,Nov 2001.
3. B.C.H. Steele, Solid State Ionics 129 (2000) 95-110.
4. Zhongliang Zhan, Ting-Lian Wen, Hengyong Tu, Zhi-Yi lu, Journal of Electrochemical Society, 148(5), A427-A432 (2001)
5. T. S. Zhang, J. Ma, L. B. Kong, S. H. Chan, J.A. Kilner, Solid State Ionics, 170 (2004) 209-217

Co-dopant Strategy

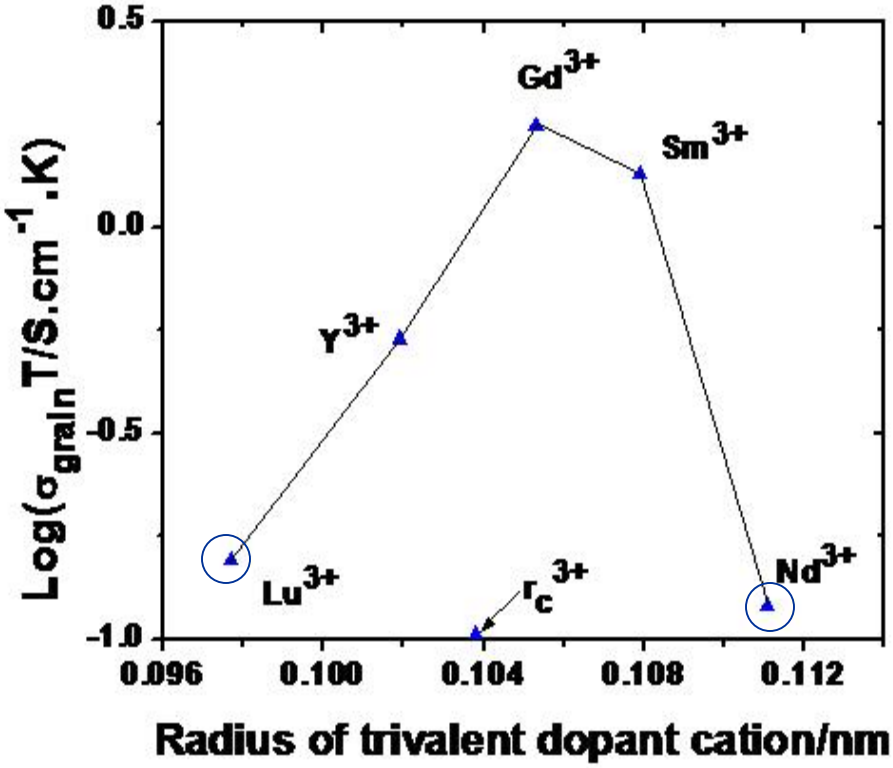

Bulk ionic conductivity at 400°C as a function of trivalent dopant radius

- Lu^{3+} and Nd^{3+} are selected as co-dopants for CeO_2 electrolyte
- They are added in proportion such that effective ionic dopant radius matches r_c^{3+}

$$Lu_xNd_yCe_{1-x-y}O_{2-\delta}$$

$$x/y = 1.16$$

To investigate the effect of polarizibility alone on the bulk ionic conductivity, Lu^{3+} doped CeO_2 was also processed.

Lu^{+3}_{VIII} = 0.977 Å
Ce^{+4}_{VIII} = 0.97 Å

X-Ray Diffraction Profile

Powder XRD profiles for different compositions of $Lu_xNd_yCe_{1-x-y}O_{2-\delta}$

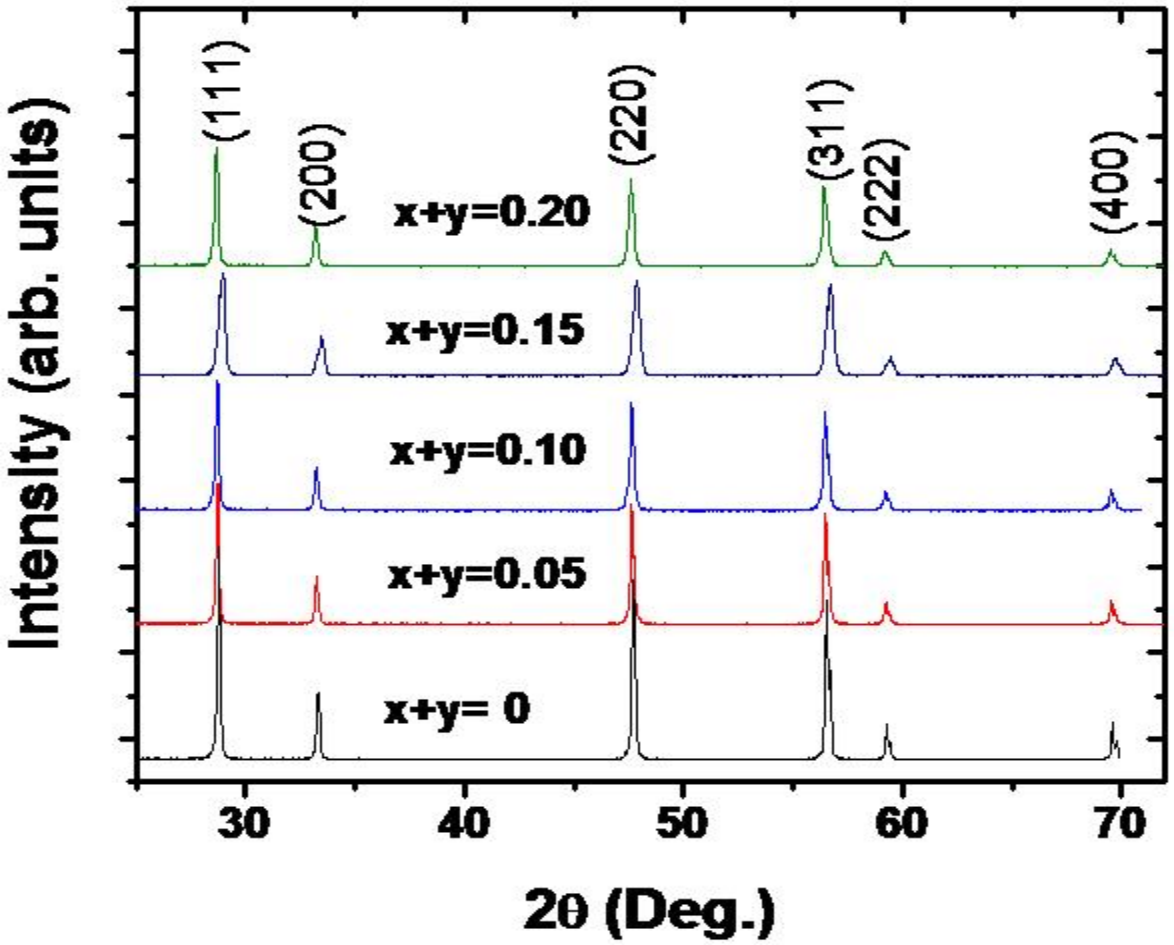

***x/y* = 1.16**

Arrhenius Plot

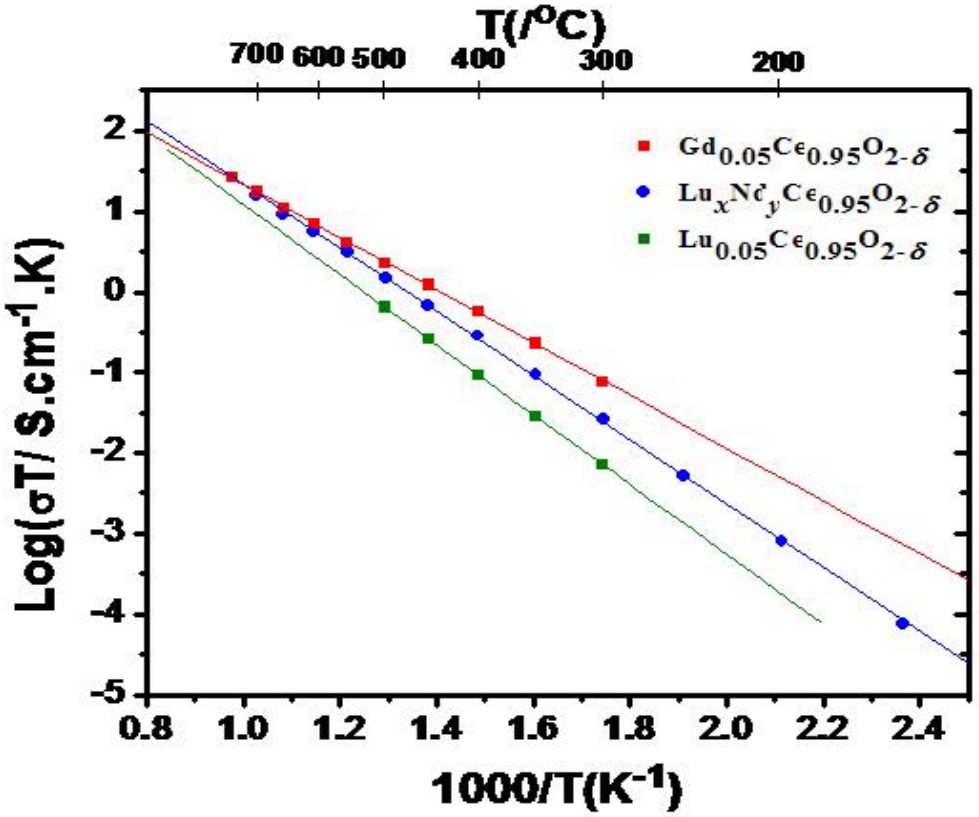

- Co-Doping Effect Works
- At 700°C $Lu_{0.027}Nd_{0.023}C_{0.95}O_{2-\delta}$ exhibits highest ionic conductivity.

***x/y* = 1.16**

Arrhenius plots for the bulk ionic conductivity of $Lu_{0.027}Nd_{0.023}Ce_{0.95}O_{2-\delta}$, $Lu_{0.05}Ce_{0.95}O_{2-\delta}$ and $Gd_{0.05}Ce_{0.95}O_{2-\delta}$ systems.

Bulk Ionic Conductivity

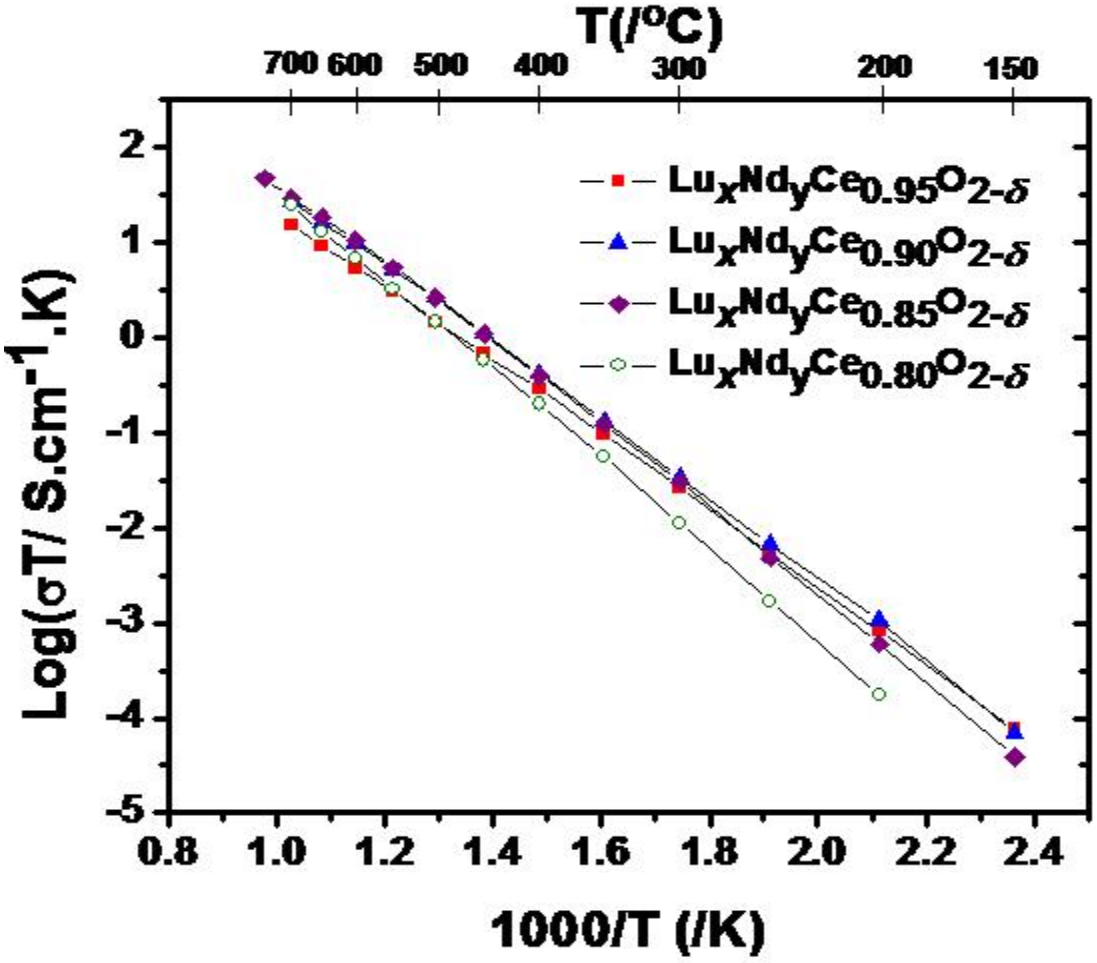

$Lu_{0.069}Nd_{0.081}Ce_{0.85}O_{2-\delta}$ exhibits the highest grain conductivity at intermediate temperatures (400°C-800°C).

***x/y* = 1.16**

Arrhenius plots for the bulk ionic conductivity of $Lu_xNd_yCe_{1-x-y}O_{2-\delta}$ system.

Bulk Ionic Conductivity

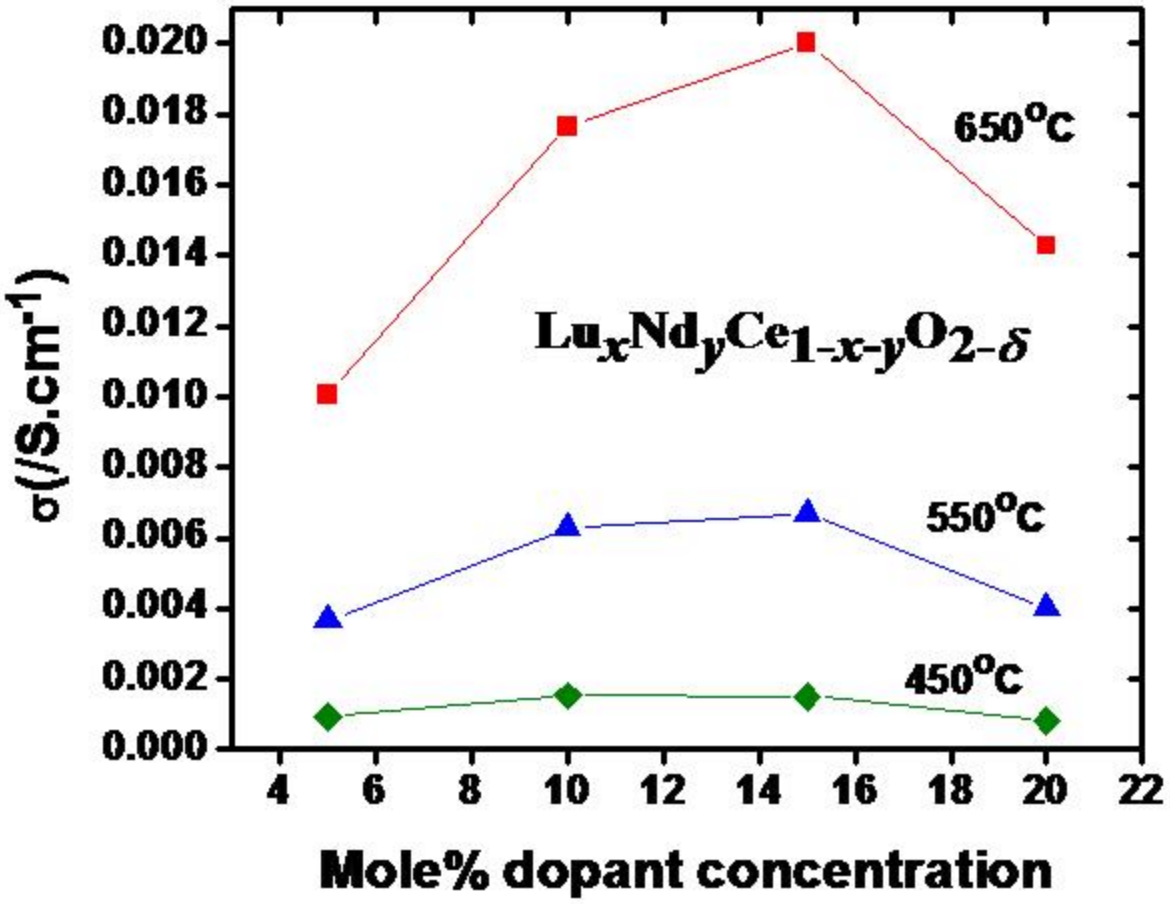

- Oxygen Vacancy formation
- Complex Defects Association formation

Bulk ionic conductivity as a function of dopant concentration (*x*+*y*)

Result

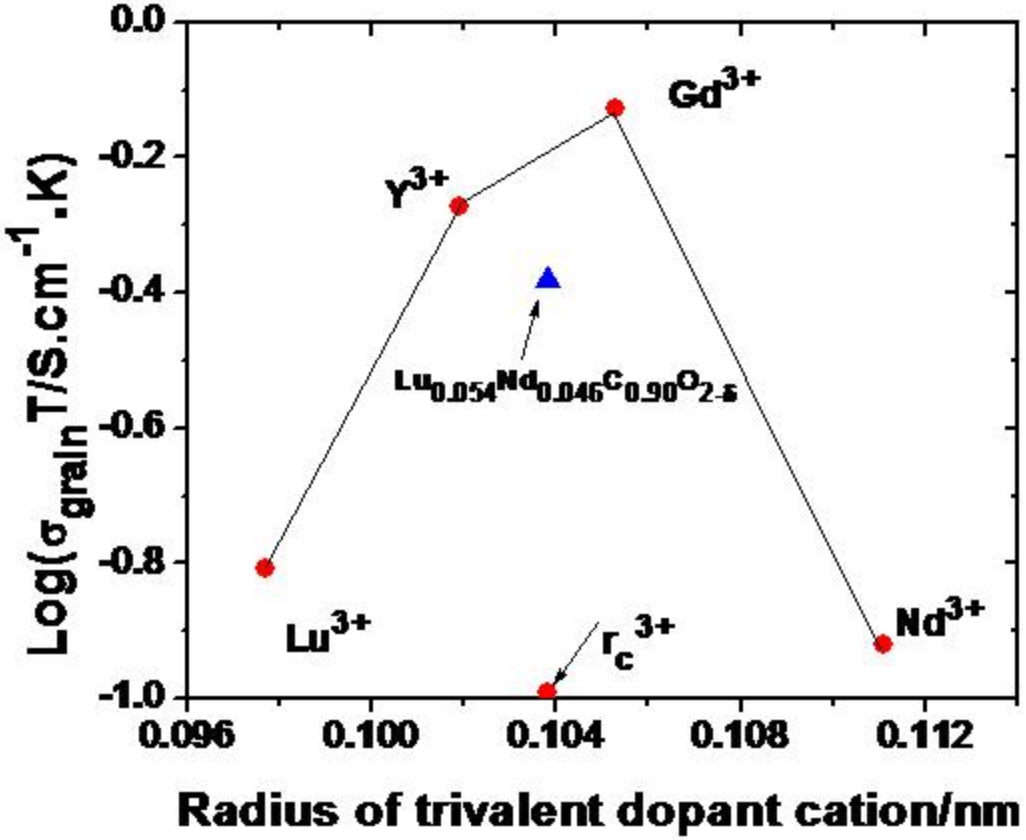

Co-dopant strategies based on critical dopant ionic radii (r_c) concept, led to increase in bulk ionic conductivity in CeO_2 based systems.

Bulk ionic conductivity at 400°C as a function of trivalent dopant radii

Future Plans

Computational

- Using "artificial dopants" of controlled size and polarizability:
  - determine the effects of dopant size of vacancy clustering
  - determine the effects of dopant polarizability on vacancy clustering
- Identify doping and co-doping strategies for mitigating effects of vacancy clustering
- Explore effects of aliovalent doping on ionic transport and vacancy clustering
- Extend to much large systems; exploit parallel simulation methods

Experimental

- Select the co-dopant based on both ionic radii and polarizibility for CeO_2 based electrolyte
- Determine conductivity of Bi_2O_3 and CeO_2 electrolytes as a function of P_{O2}
- Long term stability testing of conductivity of Bi_2O_3 and CeO_2 electrolytes